The rs1421085 variant within *FTO* promotes thermogenesis and is associated with human migration

Zhiyin Zhang
Shanghai Jiao Tong University Medical School Affiliated Ruijin Hospital
Na Chen
Shanghai Jiao Tong University Medical School Affiliated Ruijin Hospital
Ruixin Liu
Ruijin Hospital, Shanghai Jiaotong University School of Medicine https://orcid.org/0000-0002-5526-6717
Nan Yin
Shanghai Jiao Tong University Medical School Affiliated Ruijin Hospital
Yang He
Shanghai Jiao Tong University Medical School Affiliated Ruijin Hospital
Danjie Li
Shanghai Jiao Tong University Medical School Affiliated Ruijin Hospital
Muye Tong
Shanghai Jiao Tong University Medical School Affiliated Ruijin Hospital
Aibo Gao
Department of Endocrine and Metabolic Diseases, Shanghai Institute of Endocrine and Metabolic Diseases, Ruijin Hospital, Shanghai Jiao Tong University School of Medicine, Shanghai 200025
Peng Lu
National Clinical Research Center for Metabolic Diseases, Key Laboratory for Endocrine and Metabolic Diseases of Chinese Health Commission, Department of Endocrinology and Metabolism, Ruijin Hospita
Huabing Li
State key laboratory of Oncogenes and Related Genes, Shanghai Jiaotong University School of Medicine
Dan Zhang
Shengjing Hospital of China Medical University
Weiqiong Gu
National Clinical Research Center for Metabolic Diseases, Key Laboratory for Endocrine and Metabolic Diseases of Chinese Health Commission, Department of Endocrinology and Metabolism, Ruijin Hospital https://orcid.org/0000-0003-3029-1016
Jie Hong

Ruijin Hospital, Shanghai Jiao Tong University School of Medicine

Weiqing Wang

Ruijin Hospital https://orcid.org/0000-0001-6027-3084

Lu Qi

Chan School of Public Health, Boston, MA, USA

Guang Ning

Department of Endocrine and Metabolic Diseases, Shanghai Institute of Endocrine and Metabolic Diseases, Ruijin Hospital, Shanghai Jiao Tong University School of Medicine, Shanghai 200025

Jiqiu Wang (wangjq@shsmu.edu.cn)

Ruijin Hospital, Shanghai Jiao Tong University School of Medicine https://orcid.org/0000-0002-9383-7656

Article

Keywords: FTO, variant, energy expenditure, obesity, UCP1

Posted Date: October 4th, 2021

DOI: https://doi.org/10.21203/rs.3.rs-936477/v1

Version of Record: A version of this preprint was published at Nature Metabolism on July 17th, 2023. See the published version at https://doi.org/10.1038/s42255-023-00847-2.

Abstract

One lead risk signal of obesity–rs1421085 T > C within the *FTO* gene–is reported to be functional *in vitro* but lack of organismal evidence. Here, we established global and the brown-adipocyte specific locus-knock-in mice to recapitulate this homologous variant in humans and discovered that mice carrying the C-alleles showed increased thermogenic capacity and a resistance to high-fat diet-induced adiposity with enhanced FTO transcription, while FTO knockdown or inhibition effectively eliminated the increased thermogenic ability of brown adipocytes. In humans, the C-allele was associated with lower birthweight, and its allele frequency increases following the environmental temperature decreases. Cumulatively, these findings identified rs1421085 T > C as a functional variant promoting whole-body thermogenesis and was associated with early human migration from hot to cold environments.

Introduction

Following genome-wide association studies (GWAS), enormous common genetic variants in the human genome have been unraveled and proved to be associated with increasing risk of diseases development [1]. However, few of these loci show biological evidence to support their causality with diseases [1,2]. One main challenge is that most positive signals are dispersed within the noncoding regions which are less conserved among different species, hindering further functional studies using genetically modified animal models [3,4] Despite successful applications of gene editing in human cells, functional examinations at the organism level to recapitulate the specific variant in humans are still lacking [5].

To date, the largest obesity-GWAS study has revealed ~ 1000 common polymorphisms, explaining ~ 6.0% variation of body mass index (BMI) [6]. Interestingly, the positive signals repeatedly occur nearby the known monogenic obesity genes, e.g., *MC4R*, *LEPR* and *BDNF* [4]. Notably, the strongest signals of the common variants are localized within the introns of the *FTO* gene and show consistent risk-effects across multiple ethnic populations [6,7]. However, there are no evidence on *FTO* mutations causing obesity in clinical settings [8]. Loss-of-function mutations of human *FTO* are lethal owing to serious developmental defects and growth retardation [9]. Higher mortality was also observed in global *Fto* knockout mice, and the survived mice exhibited a short stature and a lean phenotype [9]. In contrast, the adipocyte-specific *Fto* knockout mice gained more body weight and showed adiposity under HFD compared with WT littermates [10]. In the past decade, the roles of *FTO* and its genetic variants in adiposity remained a topic of vigorous debate.

A turning point occurred when two research groups independently argued that certain loci (especially rs1421085) within the *FTO* variant cluster enhanced the transcription of several distal genes (including *IRX3 and IRX5*) but not *FTO per se* [11,12]. Very recently, the Nóbrega group reported the functional regulation between three additional functional *FTO* "risk variants" and the candidate genes by using a gene-editing animal model harboring 20 kb deletion of the orthologous obesity-associated interval in the *Fto* gene [13]; while the Claussnitzer and Cox groups further reported a mouse model with a deletion of 82

bp containing the homologous rs1421085 locus in *FTO* which yield a mildly lean phenotype in mice under high-fat diet (HFD) challenge [14]. Although these genetic editions contain the deletion of the *FTO* rs1421085 loci, they might also delete other potential function elements around, hence a precise knock-in mouse model of the *FTO* genetic risk loci (e.g., rs1421085_C-allele) to specifically recapitulate the human variants is still in need to understand the function of the specific risk loci.

Towards this end, we established two global and one brown adipocyte-specific single-nucleotide knock-in mouse models of the homologous human rs1421085 T > C variant, the lead functional variant in the *FTO* gene [12,15,16] (Fig. 1, A, B and K; Fig. 3A; fig. S1, A-C), and found consistent enhancement of thermogenesis and resistance to HFD-induced obesity, at least in part, by increasing FTO expression. Interestingly, the C-allele was associated with lower bodyweight of the human newborns, who have functional brown adipose tissue (BAT) as rodents do [17]. Furthermore, the C-allele frequency in multiple ethnic populations was closely related to ambient environmental temperature where they settled, with a stepwise increasing pattern from hot Africa shifting to cold Siberia.

Results

The homologous rs1421085 T > C variant promotes energy expenditure and resists HFD-induced adiposity

Evolutionary conservation around the T allele of human rs1421085 and mouse homologous loci was evaluated, which showed a high similarity (Fig. 1A**)**. To clarify the biological function of human rs1421085 T > C variant *in vivo*, a global knock-in mouse model carrying the homologous single-nucleotide mutation (the homozygous rs1421085_CC, termed KI^{cas9}) was constructed using CRISPR/Cas9 system, with wild-type (WT, rs1421085_TT) littermates as controls (Fig. 1B and fig. S1A). No significant difference on body weight gain between the two groups was observed when fed a normal chow-diet (NCD) (fig. S2A). Unexpectedly, under a HFD (60% fat) challenge, male KI^{cas9} mice gained less body weight compared with WT littermates (Fig. 1C). In agreement with the lean phenotype, KI^{cas9} mice showed an improvement of blood glucose and lipid levels as well as decrease lipid storage in the liver (fig. S2B-H). KI^{cas9} mice also had reduced total fat mass content and less inguinal white adipose tissue (iWAT) (Fig. 1D and fig. S2I). Despite no obvious alterations in food intake, physical activity, or respiratory exchange ratio (RER) (Fig. 1E; fig. S2, J and K), KI^{cas9} mice exhibited increased O_2 consumption (Fig. 1, F and G) and CO_2 production (Fig. 1, H and I), indicating a higher basal energy expenditure (Fig. 1J). We validated the HFD challenge in the following KI^{cas9} generation and gained consistent results (fig. S2L). In addition, a similar lean phenotype was also observed in female KI^{cas9} mice (fig. S2, M-Q).

To further confirm the phenotypes and exclude the possibility of off-targeted editing by CRISPR/Cas9 method, we used the conventional gene targeting strategy with homologous recombination applied to mouse embryonic stem cell (ES) to construct a second global rs1421085_CC knock-in (termed KI^{ES})

mouse model (Fig. 1K and fig. S1B). Both male and female KI^{ES} mice showed no difference in body weight as compared with control littermates under NCD (fig. S3, A and B), while showed less body weight gain, a decreased trend of fat mass and attenuated fat accumulation in liver than control littermates under HFD challenge (Fig. 1, L and M; fig. S3, C-I). These results suggested that homologous rs1421085 T > C variant resisted HFD-induced adiposity.

The homologous rs1421085 T > C variant augments the thermogenic capacity of brown adipocytes

Histological analysis showed no significant difference in the morphology of white adipose tissues between KI^{cas9} mice and WT littermates under HFD challenge (Fig. S2H). However, we observed that KI^{cas9} mice had more condensed and smaller adipocytes in BAT while WT mice showed a brown-to-white change under HFD (Fig. 2A). Consistently, the expression of thermogenesis-related genes, including *Ucp1*, *Pgc-1α*, *Prdm16*, *Cidea*, *Elov6*, *Cox7a* and *Cox8b*, were significantly increased in BAT of KI^{cas9} mice (Fig. 2B), as were the protein levels of UCP1 and PGC-1α (Fig. 2, C and D). Similar morphological changes and the increased expression patterns of these genes were further validated in BAT of KI^{ES} mice (Fig. 2, E-H; fig. S3J), together with a significant increase in mitochondrial quantity (fig. S3K). To assess the autonomous effects of homologous rs1421085 T > C variant in brown adipocyte, stromal vascular fraction (SVF) were isolated from BAT of both genotypes and induced to mature brown adipocytes [18]. An enhanced thermogenic capacity, indicated by increased thermogenesis-related genes (Fig. 2, I-K and M-O) and oxygen consumption rate (OCR) (Fig. 2, L and P), were observed in mature brown adipocytes derived from both KI^{cas9} and KI^{ES} mice models when compared with corresponding WT controls. Collectively, these results indicated that homologous rs1421085 T > C variant augmented thermogenesis of brown adipocytes both *in vivo* and *in vitro*.

Brown adipocyte-specific knock-in of homologous rs1421085 T > C variant enhances thermogenesis and resists HFD-induced adiposity

To test the hypothesis that homologous rs1421085 T > C variant in BAT might primarily contribute to the obesity-resistant phenotype, we next constructed another brown adipocyte-specific “risk allele” knock-in model by crossing homologous $rs1421085^{floxp/floxp}$ ($KI^{fl/fl}$) mice with *Ucp1*-Cre mice (*Ucp1*-Cre; $rs1421085^{floxp/floxp}$, termed *Ucp1*-$KI^{fl/fl}$) (Fig. 3A and fig. S1C). The potential interference effects of the floxp insertion *per se* on the expression of reported targets was excluded (fig. S4, A-E). Similar to the two global knock-in models, *Ucp1*-$KI^{fl/fl}$ mice showed no obvious change in body weight under NCD (fig. S4F), while displayed a resistance to HFD-induced obesity, indicated by a decrease of body weight and fat mass in comparison with control littermates (Fig. 3, B and C). Smaller lipid droplets and more mitochondria were observed in the BAT of *Ucp1*-$KI^{fl/fl}$ mice, along with a moderate improvement of lipid accumulation in liver (Fig. 3, D and E; fig. S4, G-H). In consistence, an increased expression of *Ucp1* and

other thermogenesis-related genes was observed in BAT of HFD-fed *Ucp1*-KI$^{fl/fl}$ mice (Fig. 3, F-H). Taken together, with the phenotypes of the two global and one brown adipocyte-specific knock-in models, we illustrated that the biological effect of the homologous rs1421085 T > C variant in BAT prominently contributed to the increased thermogenesis and the resistance to HFD-induced adiposity.

The homologous rs1421085 T > C variant increases thermogenesis via upregulating Fto expression

Several genes neighboring the rs1421085 locus are regarded as effective candidates of the FTO SNP cluster, e.g. *IRX3*/ *IRX5*/ *IRX6* [12], *RPGRIP1L* [10,15,19,20], and *FTO* [21,22], among which *IRX3* and *IRX5* have been shown to increase in subcutaneous preadipocytes of C-allele carriers [12]. We unbiasedly and systemically evaluated the expression of all the above genes in the BAT of three mouse models (KI^{cas9}, KI^{ES} and *Ucp1*- KI$^{fl/fl}$) and induced mature brown adipocytes of KI^{ES} mice, compared with each control. An increase of *Irx3* expression was detected in KI^{cas9} BAT (fig. S5A), and increased trends of *Irx3* expression were also observed in other KI models (fig. S5, B-D). No significant difference in other candidates was observed (despite increased trends in certain context, like *Rpgrip1l* in KI^{ES} BAT) (fig. S5, A-D). Importantly, moderate and sustainable elevation of *Fto* expression was detected in both mRNA and protein levels in each KI model (Fig. 4, A-C). Indeed, the 1 kb genome region containing the “risk allele” of rs1421085 (as well as rs9940128 and rs11642015) showed higher enhancer activity than the major allele [12,13]; however, the downstream target-promoter of these variants has not been clarified. In this regard, four reporter plasmids carrying the 1 kb human genome fragments centered on rs1420185 (T and C allele, respectively) inserted ahead of the human *FTO* promoter (h*FTO*p) sequence either in a forward direction (5' to 3') or reverse direction (3' to 5'), were constructed to investigate the direct enhancer effect of this variant on the activity of *FTO* promoter *per se* (Fig. 4D). When linked in a reverse direction, the major allele (T) 1-kb genome fragment enhanced the transcription activity of *FTO* promoter, and the “risk allele (C)” genome fragment further advanced the activity. This phenomenon did not occur once the fragments were arranged in a forward direction ahead of the promoter (Fig. 4E).

The biological role of FTO in brown adipocytes remains elusive [10]. We found that during the *in vitro* differentiation of brown adipocytes, *Fto* expression increased continuously, in parallel with the increase pattern of thermogenesis-related genes such as *Ucp1* and *Pgc-1α* (fig. S6A). A strong positive linear correlation between *Fto* and *Ucp1* mRNA expression was observed (fig. S6B). Of importance, *Fto* knock-down reduced the mRNA and protein expression of *Ucp1* and other thermogenesis-related genes remarkably, and *Fto* deficiency impaired the thermogenic capacity of induced brown adipocytes in a dose-dependent manner (Fig. 4, F-H; fig. S6, C-E); meanwhile *Fto* overexpression increased their expression (Fig. 4I-K; fig. S6F). Moreover, entacapone (ENT), which acts as an m6A demethylation inhibitor of FTO protein, resulted in impairment of *Ucp1* expression in the induced brown adipocytes (fig. S6, G-J). These results suggested that FTO protein positively regulated *Ucp1* expression in brown adipocytes.

To better illustrate the role of FTO in functional BAT pads, and to avoid the secondary interference of growth defects observed in global *Fto* knockout mice [3], we crossed *Fto*$^{floxp/floxp}$ mice with *Myf5*-Cre mice [23] to delete *Fto* in BAT (*Myf5*-Cre;*Fto*$^{floxp/floxp}$, termed MFKO) (fig. S7A). Under HFD challenge, MFKO mice showed an increased body weight gain (fig. S7, B and C) and a decline of energy expenditure as compared with control mice (fig. S7, D-K). Of importance, *ex vivo* experiments showed that UCP1 protein expression decreased upon FTO deletion in the induced brown adipocytes from MFKO mice (fig. S7, L and M).

We further performed RNA immunoprecipitation followed by qPCR (RIP-qPCR) and agarose gel electrophoresis (AGE) tests, and observed that endogenous FTO protein bound to *Ucp1* mRNA in mature brown adipocytes (fig. S8, A-C). We also observed an interaction of FTO protein with *C/ebpa* mRNA (fig. S8, B and D), consistent with previous findings in NOMO-1 cells [24]. Moreover, FTO deficiency significantly reduced the stability of *Ucp1* transcripts while merely affect that of *C/ebpa*, suggesting that *Ucp1* was one main target of FTO protein in mature brown adipocytes (fig. S8, E and F). Importantly, the increased *Ucp1* expression and enhanced OCR of KI^{ES} brown adipocytes was greatly repressed with either silence of *Fto* gene or enzymic inhibition of FTO protein (Fig. 4, L-O; fig. S8, G-H). We noticed an incomplete elimination of the differences between groups, which indicated that other downstream genes of the variant (like *Irx3*[12]) might also be involved in the process [25,26]. Taken together, these findings revealed that the effects of the homologous rs1421085 T > C variant on the increasing thermogenesis and *Ucp1* expression depended largely on the FTO protein.

The rs1421085 T > C variant is associated with lower body weight of human infants and its allele frequency parallels with latitudes and ambient temperature of population distribution

Rodents possess thermo-active BAT throughout life, whereas in humans BAT activation peaks after birth to combat the extrauterine coldness for survival and then vanishes with growth [27]. To evaluate the potential contribution of BAT degeneration on the adiposity-related outcomes of rs1421085 T > C variant, we surgically removed intrascapular BAT (iBAT) by iBAT excision (△iBAT) [28] in KI^{cas9} and WT littermates (fig. S9A). Without iBAT, KI^{cas9} mice lost adiposity resistance under HFD; on the contrary, they appeared to have more body weight increase, higher fat mass percentage, larger white adipocytes and more severe ectopic lipid deposition in the liver when compared to controls (fig. S9, B-F), in agreement with the adiposity traits of the adult humans carrying the “risk-allele”.

Given the substantial biological effects of homologous rs1421085 T > C variant on murine BAT function and adiposity, we hypothesized that rs1421085 T > C variant may associate with a lower body weight in humans carrying functional BAT. Indeed, a few well-designed longitudinal studies have indicated that the association between *FTO* SNPs and body weight changes dynamically with growth [29]. Thus, we performed a meta-analysis to explore the effect of *FTO* polymorphism (including rs1421085 and other three linkage disequilibrium SNPs) on body weight/BMI. In agreement with previous findings [30–38], BMI difference between the effect (minor)-allele and the reference (major)-allele groups emerged since about 8

years old, as a higher average BMI was observed in the effect-allele group (fig. S10A); this difference disappeared when the included population was restricted to younger than 8 years old (fig. S10B). Importantly, we observed a mild but significant decrease of birth weight in the effect-allele group (P = 0.009, 95% CI: [-0.11, -0.02]; Fig. 5A). As only a few of studies described the histological and molecular characteristics of human fetal BAT [39], we collected fetal BAT and confirmed the existence of functional BAT even at middle-gestational stage (fig. S11). In further, we found the co-localization of FTO and UCP1 protein in fetal brown adipocytes featured with strong UCP1 and PLIN1 staining (fig. S11), suggesting a potential role of FTO in fetal BAT development and human thermogenesis.

Although a strong positive association between *FTO* SNPs (including rs1421085) and obesity is confirmed across adult populations of diverse ancestry, a relatively weaker association and a lower frequency of "risk alleles" have been observed according to large-scale GWAS studies based on African populations [16,40,41]. To date, reasons for the discrepancy among African and non-African populations remains unclarified. Herein, we assumed that environmental coldness, which activates BAT but rarely occurred in Africa, might contribute to the low frequency distribution of the *FTO* variants. To this end, we first analyzed ambient environmental temperatures with the allele frequency of the rs1421085 T > C variant in various populations (of all the 1000 Genomes populations, see **Methods**), and observed a significantly inverse correlation in populations settled in Africa-Eurasian continents ($P = 0.0001$, $R^2 = -0.33$; Fig. 5B). The inverse correlation remained significant after adjusting Paleozoic temperature (which possibly affected BAT function in ancient humans) using two published models [42] ($P < 0.0001$, $R^2 = -0.40$, and $P < 0.0001$, $R^2 = -0.39$, respectively; fig. S12, A and B). In addition, we analyzed the correlation between the variant frequency and the coordinates latitudes (one determinant factor of ambient environment temperature) of all populations and observed a more robust positive association ($P < 0.0001$, $R^2 = 0.48$) (Fig. 5C). Meanwhile, no statistically significant correlation was found between the variant frequency and longitudes or altitudes among populations (fig. S12, C and D).

Adaption to coldness outside Africa, especially during the last ice age, was a major challenge for early Homo sapiens migrating from East Africa [43]. Acclimatization through genetic accommodation during human migration is a prevailing theory, e.g. the $EDAR^{V370A}$ mutation selected by warm and humid Asia environment [44], the unique EPAS1 haplotype structure selected by the hypoxic environment of the high-altitude Tibetan platens [45]. From this aspect, with modern humans leaving Africa, migrating, and finally settling on other continents, their ambient temperature/residential location shifted from a warm/low latitude to cold/high latitude. While referring to human migration route maps reported by previous studies [46], we proposed a genetic diffusion map of the rs1421085 T > C variant frequency on the African and the Eurasian continents, that is, the frequency was lowest in East Africa, intermediate in East and South Asia, increased in Europe, and finally reached its zenith in Siberia (Fig. 5D).

Discussion

Immediately after the identification of the association between FTO variants and obesity, Palmer's group made an elegant and well-controlled comparison of the energy balance of FTO "risk allele" carriers versus non-carriers in 4–10 years old children [47]. An indirect calorimetry approach was applied to assess basal metabolic rate (BMR), while the doubly labeled water method (used as golden standard [48]) was employed to measure total energy expenditure. Paradoxically, they revealed that the "risk allele" carriers had a higher BMR and total energy expenditure than non-carriers. Nevertheless, despite that covariate adjustment partially abolished the "risk allele" effects on BMR, the total energy expenditure remained significantly different between the two groups (an increase of 1160 kJ in "risk-allele" carriers). Unfortunately, these important findings were ignored as subsequent studies overwhelmingly argued that the "risk allele" had no or a reduction effect on energy expenditure in adults [12,49]. The causal effects of the FTO risk allele at the organism level remain to be illusive. It is emphasized that humanized murine models are powerful tools to dissect mechanisms underlying the association of FTO variants with human phenotypes [50,51]. To our knowledge, to date, there is no report regarding murine models to exactly recapitulate human FTO polymorphisms with single-nucleotide substitution methods. Towards this end, we initially established two strains of global homologous rs1421085 T > C variant knock-in mice using CRISPR/Cas9 and conventional gene-targeting with homologous recombination strategies, respectively. A third strain of brown adipocyte-specific homologous C-allele single-point knock-in mice was constructed to confirm its biological roles in BAT. In support of Palmer's findings in children [47], our study reported the FTO variant yielded an enhancement of thermogenic gene expression, oxygen consumption, and total energy expenditure of brown adipocytes both *in vivo* and *ex vivo*. Another important finding is that the rs1421085 T > C variant is indeed a pivotal genetic trigger modulating a line of downstream genes, among which *Fto* showed the most stably increased expression in "risk-allele" group. Furthermore, we provided a reliable evidence of FTO protein directly regulating *Ucp1* expression both *in vivo* and *in vitro*, which was consistent with the obese phenotype observed in adipocyte-specific *Fto* knockout mice [10], pointing out the involvement of FTO in the function of the rs1421085 T > C variant. Except for *Fto*, we also validated an increased expression of *Irx3*, *Irx5* [11–13] and *Rpgrip1l* [15] in certain contexts, supporting a temporal, spatial, and cell type-dependent regulation by the variant [13]. Furthermore, we have previously revealed that IRX3 overexpression promoted the transcriptional activity of *Ucp1* and enhanced thermogenesis in brown adipocytes [25,26], which might be one plausible explanation for the incomplete rescue of FTO knockdown or inhibition to the rs1421085 T > C variant's effects. We want to mention that these findings in the knock-in models of this single-nucleotide variant is not completely the same as in the recently reported two mouse models harboring a deletion of 82 bp and 20 kb containing the same FTO variant, respectively [13,14], which may be due to non-specific deletion of other potential functional motifs in the region by their strategies. Our models that recapitulate the same human variant are more specific for the evaluation of the pathophysiological changes produced by the homologous rs1421085 T > C variation at the organism level.

The first available document about BAT deposition in infants was reported by Neumann in 1902 [52]. BAT in human newborn infants produces heat by non-shivering thermogenesis to maintain body temperature.

When the infants were shifted from 34–35℃ (thermoneutral temperature) to 25–26℃ (cooling temperature), their rectal temperature dropped 0.1–0.5℃ and O_2 consumption almost doubled, accompanied by a relatively warmer skin temperature of the intrascapular BAT region than other sites [53]. BAT depletion or BAT functional defects are associated with the development of “cold syndrome”, which threatens newborn infants’ survival [54]. These phenomena gave rise to speculation that higher BAT content or activity would increase the survival of infants born in ambient cold temperatures. For example, the Last Glacial Maximum (LGM), when the mean temperature was 6.1℃ lower than nowadays [55], challenged all species including modern humans. Some species adapted to the prehistoric climate successfully [56], while others, e.g., archaic humans, *Neanderthals*, *Denisovans*, and *Homo erectus*, became extinct [57]. To date, factors that determine such successful adaptation are still poorly understood [58,59]. We found that rs1421085 T > C knock-in increased the thermogenic capacity of mice. In this context, the functional FTO variant–rs1421085 T > C–has likely increased the survival odds of human newborn infants by increasing their thermogenesis. In consistent with this hypothesis, we found that the frequency of rs1421085 T > C was the lowest in East and Middle Africa, higher in East Europe, much higher in North Europe, and reached the highest in Siberia. Interestingly, the association between the FTO variants and obesity in European and Asian populations is not well-validated in Africans, and only mild effect was observed in a few studies [16,40,41]. Furthermore, a tight linkage disequilibrium among various obesity-related GWAS positive signals that clustered within the first intron of the *FTO* gene is observed in non-African populations, while this genetic architecture of the FTO loci breaks down in native Africans [16]. These findings suggest that this genomic region has experienced genomic recombination and undergone genetic selection since modern humans descended from several branches of Homo sapiens populations that migrated out of Africa [40]. Several possibilities exist regarding the origin and distinct distribution frequency of the rs1421085 T > C variant between Africans and non-Africans. One hypothesis is that the variant arose occasionally in African populations, and after encountering extremely cold temperatures during the migration away from Africa, those newborns carrying the variant gained higher thermogenic capacity to thrive. The frequency subsequently increased stepwise, in parallel with migration, which started in the hot/low latitudes and gradually increased when moving to the cold/high latitudes. Another hypothesis claims that, in cold temperatures, an intense genomic recombination within the first intron of the *FTO* gene induced random occurrence of rs1421085 T > C in a variety of populations, independently. Populations in Africa rarely encountered such cold exposure, thus the variant was merely observed. According to this hypothesis, the rs1421085 T > C variant first presented in archaic humans after they settled in Eurasia, later the genomic fragment containing the variant possibly flowed back to Africa. This process might have happened repeatedly [60]. It should be pointed out that all these possibilities warrant further genetic evidence of modern and archaic humans for confirmation or exclusion. Of note, a few nucleotide sequences centered to the rs1421085 locus were reported to be transcription factor (e.g., ARID5B and CUX1 [12,15]) -binding elements, showing a high conservation among species, even including zebrafish [12]. These results indicate the *cis*-elements might be essential for the expression of downstream targets, while our data support that the T > C alteration belongs to a gain-of-function mutation. In future studies, element disruption at the locus would be informative for us to understand the roles of wild-type

genotypes in obesity and other pleiotropic outcomes. Despite that BAT brought evolutionary advantages for mammals to survive cold stress [61,62], whether the thermogenic variation contributes to natural selection in the evolution of mammalian endothermy is also a matter of uncertainty [63]. It should be noted that, in additional to the rs1421085 T > C variant, other FTO variants also have functional impacts on the target genes [13,15]. The various haplotypes at convergence of different variants would lead to fluctuation of the phenotypes, including energy expenditure and appetite [64].

On the other hand, how to re-evaluate the predisposition of the “risk-allele” to adiposity in adult humans? According to the Early Growth Genetics (EGG) Consortium data, a shift pattern of the effect of the *FTO* rs9939609 T > A variant on BMI was observed in adolescents of different ages: with a positive association between the “risk allele” and BMI from 5.5 years old onwards; however, there was an inverse association below 2.5 years old [29]. In consistence, the genetic influence of the same variant (rs9939609) on BMI was progressively stronger with increasing age (from 0.48 at 4y to 0.78 at 11y), as reported from a longitudinal large twin cohort of more than 7,000 children [65], which further indicated an age-related characteristic of FTO variants in the regulation of adiposity. In humans, BAT diminishes rapidly in the first decade of life [17,66]. To test whether this disappearance influence the biological effect of *Fto* variant on adiposity phenotypes, we removed intrascapular BAT of both KI^{ES} and WT mice, and successfully simulated the predisposition of the “risk allele” to obesity, as observed in humans. This interesting finding provided some potential underlying explanations for the phenotype shift from obesity-resistance to obesity-sensitivity of the rs1421085 T > C variant, such as the compensatory role of this variant in other tissues in addition to BAT (e.g., hypothalamus and WAT), the reduction of certain metabolic-protective secretory factors (e.g., BMP8b, FGF21 and IL-6) of BAT [67], or the long-term consequence of altered feeding/eating habits at early life and following catch-up growth [68]. In a further speculation, other potential downstream targets of rs1421084 T > C, e.g., *IRX3*/ *IRX5*/ *IRX6* [12,13] and *RPGRIP1L* [15], as well as the target of *FTO per se* [69], could also participate in the compensatory predisposition to adiposity.

Conclusion

In summary, by collecting evidence from population studies as well as genetically modified murine models, we uncovered the possible biological roles and molecular basis of the rs1421085 T > C variant and postulated the rs1421085 T > C– *Fto*– *Ucp1* axis in the regulation of BAT thermogenesis. These findings may enhance our understanding regarding the possible “causative biological functions” of the “risk variants” derived from extensive GWAS data especially for those localized in non-coding regions and further remind us of the importance of genome-environment interaction, and the potential contribution of genetic variants in the process of adaptive evolution.

Declarations

Acknowledgments: We thank all the participants for their involvements in this study, and we thank Dr. Juan Shen and Dr. Qijun Liao from BGI-Shenzhen for their suggestive comments on adaptive evolution of

the FTO variant.

Funding: This work was supported by grants from the National Natural Science Foundation of China (91957124, 91857205, 81822009, 82088102, 82050007, 81730023, 81930021, and 81870585), National Key Research and Development Program of China (2018YFC1313802), Shanghai Municipal Education Commission-Gaofeng Clinical Medicine Grant Support (20161306 and 20171903), the Outstanding Academic Leader Program of Shanghai Municipal Health Commission (2018BR01), and Program of Shanghai Academic/Technology Research Leader (20XD1403200).

Author contributions: J.W. and G.N. designed the experiments and supervised the study. Z.Z., N.C., N.Y., and Y.H. carried out the animal and molecular experiments. J.W., N.Y., and M.T. analyzed the genetic data. J.W. and R.L. analyzed all the experimental data. D.L, A.G., P.L., and H.L. provided supports in animal model tests. G.N., W.W., J.H., W.G.., and W.W. provided the cohort resources. J.W., R.L., and Z.Z. wrote the manuscript. L.Q. contributed to text revision and discussion.

Declaration of Interests

The authors declare no competing interests.

References

1. Claussnitzer, M. *et al.* A brief history of human disease genetics. *Nature* **577**, 179–189 (2020).
2. Wijmenga, C. & Zhernakova, A. The importance of cohort studies in the post-GWAS era. *Nat. Genet.* **50**, 322–328 (2018).
3. McMurray, F. *et al.* Adult Onset Global Loss of the Fto Gene Alters Body Composition and Metabolism in the Mouse. *PLoS Genet.* **9**, (2013).
4. Van Der Klaauw, A. A. & Farooqi, I. S. The hunger genes: Pathways to obesity. *Cell* **161**, 119–132 (2015).
5. Zhu, F., Nair, R. R., Fisher, E. M. C. & Cunningham, T. J. Humanising the mouse genome piece by piece. *Nat. Commun.* **10**, 1–13 (2019).
6. Yengo, L. *et al.* Meta-analysis of genome-wide association studies for height and body mass index in ~700000 individuals of European ancestry. *Hum. Mol. Genet.* **27**, 3641–3649 (2018).
7. Locke, A. E. *et al.* Genetic studies of body mass index yield new insights for obesity biology. *Nature* **518**, 197–206 (2015).

8. Meyre, D. *et al.* Prevalence of loss-of-function FTO mutations in lean and obese individuals. *Diabetes* **59**, 311–318 (2010).
9. Fischer, J. *et al.* Inactivation of the Fto gene protects from obesity. *Nature* **458**, 894–898 (2009).
10. Wang, C.-Y. *et al.* Loss of FTO in adipose tissue decreases Angptl4 translation and alters triglyceride metabolism. *Science signaling* **8**, ra127 (2015).
11. Smemo, S. *et al.* Obesity-associated variants within FTO form long-range functional connections with IRX3 Scott. *Nature* **507**, 371–375 (2014).
12. Claussnitzer, M. *et al.* FTO obesity variant circuitry and adipocyte browning in humans. *N. Engl. J. Med.* **373**, 895–907 (2015).
13. Sobreira, D. R. *et al.* Extensive pleiotropism and allelic heterogeneity mediate metabolic effects of IRX3 and IRX5. *Science* **372**, 1085–1091 (2021).
14. Laber, S. *et al.* Linking the FTO obesity rs1421085 variant circuitry to cellular, metabolic, and organismal phenotypes in vivo. *Sci. Adv.* **7**(**30**), (2021).
15. Stratigopoulos, G. *et al.* Hypomorphism of Fto and Rpgrip1l causes obesity in mice. *J. Clin. Invest.* **126**, 1897–1910 (2016).
16. Peters, U. *et al.* A systematic mapping approach of 16q12.2/FTO and BMI in more than 20,000 African Americans narrows in on the underlying functional variation: results from the Population Architecture using Genomics and Epidemiology (PAGE) study. *PLoS Genet.* **9**, e1003171 (2013).
17. Lean, M. E., James, W. P., Jennings, G. & Trayhurn, P. Brown adipose tissue uncoupling protein content in human infants, children and adults. *Clin. Sci. (Lond).* **71**, 291–297 (1986).
18. Wang, J. *et al.* Ablation of LGR4 Promotes Energy Expenditure by Driving White-To-Brown Fat Switch. *Nat. Cell Biol.* **15**, 1455–1463 (2013).
19. Stratigopoulos, G., LeDuc, C. A., Cremona, M. L., Chung, W. K. & Leibel, R. L. Cut-like homeobox 1 (CUX1) regulates expression of the fat mass and obesity-associated and retinitis pigmentosa GTPase regulator-interacting protein-1-like (RPGRIP1L) genes and coordinates leptin receptor signaling. *J. Biol. Chem.* **286**, 2155–2170 (2011).
20. Tung, Y. C. L., Yeo, G. S. H., O'Rahilly, S. & Coll, A. P. Obesity and FTO: Changing focus at a complex locus. *Cell Metab.* **20**, 710–718 (2014).
21. Grunnet, L. G. *et al.* Regulation and function of FTO mRNA expression in human skeletal muscle and subcutaneous adipose tissue. *Diabetes* **58**, 2402–2408 (2009).
22. Klöting, N. *et al.* Inverse relationship between obesity and FTO gene expression in visceral adipose tissue in humans. *Diabetologia* **51**, 641–647 (2008).
23. Schulz, T. J. *et al.* Brown-fat paucity due to impaired BMP signalling induces compensatory browning of white fat. *Nature* **495**, 379–383 (2013).
24. Su, R. *et al.* Targeting FTO Suppresses Cancer Stem Cell Maintenance and Immune Evasion. *Cancer Cell* 1–18 (2020). doi:10.1016/j.ccell.2020.04.017

25. Zhang, Z. *et al.* IRX3 Overexpression Enhances Ucp1 Expression In Vivo. *Front. Endocrinol. (Lausanne).* **12**, 634191 (2021).
26. Zou, Y. *et al.* IRX3 Promotes the Browning of White Adipocytes and Its Rare Variants are Associated with Human Obesity Risk. *EBioMedicine* **24**, 64–75 (2017).
27. Symonds, M. E., Mostyn, A., Pearce, S., Budge, H. & Stephenson, T. Endocrine and nutritional regulation of fetal adipose tissue development. *J. Endocrinol.* **179**, 293–299 (2003).
28. Grunewald, Z. I. *et al.* Removal of interscapular brown adipose tissue increases aortic stiffness despite normal systemic glucose metabolism in mice. *Am. J. Physiol. - Regul. Integr. Comp. Physiol.* **314**, R584–R597 (2018).
29. Sovio, U. *et al.* Association between common variation at the FTO locus and changes in body mass index from infancy to late childhood: the complex nature of genetic association through growth and development. *PLoS Genet.* **7**, e1001307 (2011).
30. Pausova, Z. *et al.* A common variant of the FTO gene is associated with not only increased adiposity but also elevated blood pressure in french canadians. *Circ. Cardiovasc. Genet.* **2**, 260–269 (2009).
31. Hakanen, M. *et al.* FTO genotype is associated with body mass index after the age of seven years but not with energy intake or leisure-time physical activity. *J. Clin. Endocrinol. Metab.* **94**, 1281–1287 (2009).
32. Fang, H. *et al.* Variant rs9939609 in the FTO gene is associated with body mass index among Chinese children. *BMC Med. Genet.* **11**, (2010).
33. Xi, B. *et al.* The common rs9939609 variant of the fat mass and obesity-associated gene is associated with obesity risk in children and adolescents of Beijing, China. *BMC Med. Genet.* **11**, (2010).
34. Liu, G. *et al.* FTO variant rs9939609 is associated with body mass index and waist circumference, but not with energy intake or physical activity in European- and African-American youth. *BMC Med. Genet.* **11**, (2010).
35. Scott, R. A. *et al.* FTO genotype and adiposity in children: Physical activity levels influence the effect of the risk genotype in adolescent males. *Eur. J. Hum. Genet.* **18**, 1339–1343 (2010).
36. Seal, N., Weaver, M. & Best, L. G. Correlates of the FTO gene variant (rs9939609) and growth of American Indian infants. *Genet. Test. Mol. Biomarkers* **15**, 633–638 (2011).
37. Mook-Kanamori, D. O. *et al.* No association of obesity gene FTO with body composition at the age of 6 months. The Generation R Study. *J. Endocrinol. Invest.* **34**, 16–20 (2011).
38. Lauria, F. *et al.* Prospective Analysis of the Association of a Common Variant of FTO (rs9939609) with Adiposity in Children: Results of the IDEFICS Study. *PLoS One* **7**, (2012).
39. Velickovic, K. *et al.* Expression and subcellular localization of estrogen receptors α and β in human fetal brown adipose tissue. *J. Clin. Endocrinol. Metab.* **99**, 151–159 (2014).
40. Loos, R. J. F. & Yeo, G. S. H. The bigger picture of FTO: the first GWAS-identified obesity gene. *Nat. Rev. Endocrinol.* **10**, 51–61 (2014).

41. Monda, K. L. *et al.* A meta-analysis identifies new loci associated with body mass index in individuals of African ancestry. *Nat. Genet.* **45**, 690–696 (2013).
42. Eisenberg, D. T. A., Kuzawa, C. W. & Hayes, M. G. Worldwide allele frequencies of the human apolipoprotein E gene: climate, local adaptations, and evolutionary history. *Am. J. Phys. Anthropol.* **143**, 100–111 (2010).
43. Clemente, F. J. *et al.* A selective sweep on a deleterious mutation in CPT1A in Arctic populations. *Am. J. Hum. Genet.* **95**, 584–589 (2014).
44. Kamberov, Y. G. *et al.* Modeling recent human evolution in mice by expression of a selected EDAR variant. *Cell* **152**, 691–702 (2013).
45. Huerta-Sánchez, E. *et al.* Altitude adaptation in Tibetans caused by introgression of Denisovan-like DNA. *Nature* **512**, 194–197 (2014).
46. Nielsen, R. *et al.* Tracing the peopling of the world through genomics. *Nature* **541**, 302–310 (2017).
47. Cecil, J. E., Tavendale, R., Watt, P., Hetherington, M. M. & Palmer, C. N. A. An obesity-associated FTO gene variant and increased energy intake in children. *N. Engl. J. Med.* **359**, 2558–2566 (2008).
48. Nagy, K. A. Doubly labeled water method (3 HH 18 O): a guide to its use. 1–45 (1983).
49. Speakman, J. R., Rance, K. A. & Johnstone, A. M. Polymorphisms of the FTO gene are associated with variation in energy intake, but not energy expenditure. *Obesity* **16**, 1961–1965 (2008).
50. Herman, M. A. & Rosen, E. D. Making biological sense of GWAS data: Lessons from the FTO locus. *Cell Metab.* **22**, 538–539 (2015).
51. O'Rahilly, S., Coll, A. P. & Yeo, G. S. H. FTO Obesity Variant and Adipocyte Browning in Humans. *The New England journal of medicine* **374**, 191 (2016).
52. Ravussin, E. & E.Galgani, J. The Implication of Brown Adipose Tissue for Humans. *Annu Rev Nutr.* 33–47 (2011). doi:10.1146/annurev-nutr-072610-145209
53. Dawkins, M. J. & Scopes, J. W. Non-shivering thermogenesis and brown adipose tissue in the human new-born infant. *Nature* **206**, 201–202 (1965).
54. Marsh, A. R. A short but distant war - The Falklands Campaign. *J. R. Soc. Med.* **76**, 972–982 (1983).
55. Tierney, J. E. *et al.* Glacial cooling and climate sensitivity revisited. *Nature* **584**, 569–573 (2020).
56. Kumar, V., Kutschera, V. E., Nilsson, M. A. & Janke, A. Genetic signatures of adaptation revealed from transcriptome sequencing of Arctic and red foxes. *BMC Genomics* **16**, 585 (2015).
57. Stewart, J. R. & Stringer, C. B. Human evolution out of Africa: the role of refugia and climate change. *Science* **335**, 1317–1321 (2012).
58. Enerbäck, S. Human brown adipose tissue. *Cell Metab.* **11**, 248–252 (2010).
59. Dibble, H. L. *et al.* How did hominins adapt to ice age Europe without fire? *Curr. Anthropol.* **58**, S278–S287 (2017).
60. Henn, B. M. *et al.* Genomic ancestry of North Africans supports back-to-Africa migrations. *PLoS Genet.* **8**, (2012).

61. Cannon, B. & Nedergaard, J. Brown adipose tissue: function and physiological significance. *Physiol. Rev.* **84**, 277–359 (2004).
62. Smith, R. E. & Roberts, J. C. THERMOGENESIS OF BROWN ADIPOSE TISSUE IN COLD-ACCLIMATED RATS. *Am. J. Physiol.* **206**, 143–148 (1964).
63. Jastroch, M., Oelkrug, R. & Keipert, S. Insights into brown adipose tissue evolution and function from non-model organisms. *J. Exp. Biol.* **221**, (2018).
64. Harbron, J., van der Merwe, L., Zaahl, M. G., Kotze, M. J. & Senekal, M. Fat mass and obesity-associated (FTO) gene polymorphisms are associated with physical activity, food intake, eating behaviors, psychological health, and modeled change in body mass index in overweight/obese Caucasian adults. *Nutrients* **6**, 3130–3152 (2014).
65. Haworth, C. M. A. *et al.* Increasing heritability of BMI and stronger associations with the FTO gene over childhood. *Obesity (Silver Spring).* **16**, 2663–2668 (2008).
66. Heaton, J. M. The distribution of brown adipose tissue in the human. *J. Anat.* **112**, 35–39 (1972).
67. Villarroya, F., Cereijo, R., Villarroya, J. & Giralt, M. Brown adipose tissue as a secretory organ. *Nat. Rev. Endocrinol.* **13**, 26–35 (2017).
68. Reilly, J. J. *et al.* Early life risk factors for obesity in childhood: cohort study. *BMJ* **330**, 1357 (2005).
69. Li, Z. *et al.* FTO Plays an Oncogenic Role in Acute Myeloid Leukemia as a N6-Methyladenosine RNA Demethylase. *Cancer Cell* **31**, 127–141 (2017).

Figures

Figure 1

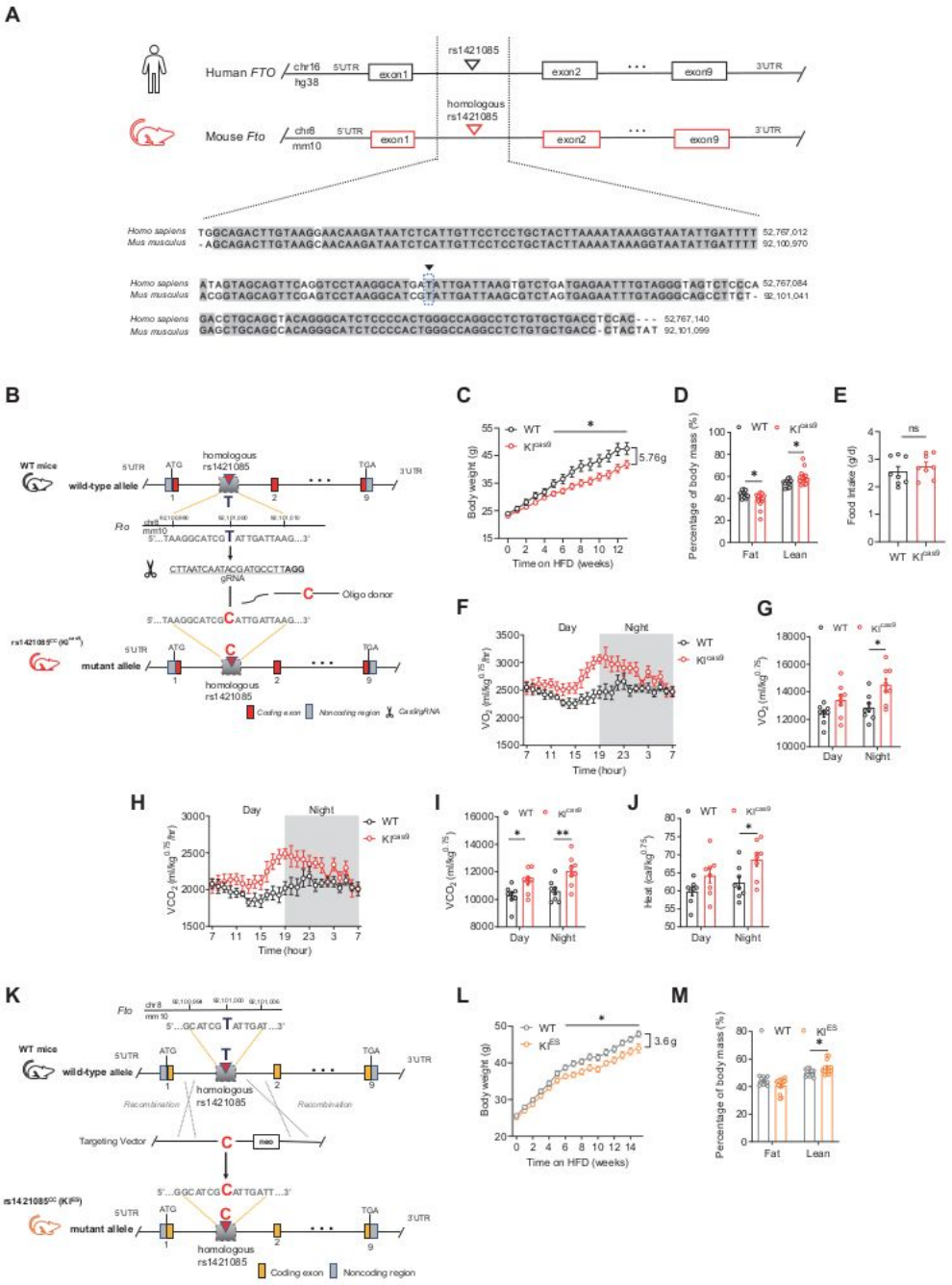

Figure 1

The homologous rs1421085 T>C variant promotes energy expenditure and resists HFD-induced adiposity. (A) Schematic diagram of the construction of the homologous rs1421085_C knock-in (KIcas9) mouse model with CRISPR/Cas9 method. (B to D) Body weight (B), body composition (C), and food intake (D) of KIcas9 mice and WT littermates under HFD challenge initiating from 8-week-old to 21-week-old (B, C, n = 11:16, D, n=8:8). (E to I) Whole-day and 12h O2 consumption rates (E-F), CO2 production rates (G-H), and

heat generation (I) of KIcas9 and WT mice were measured at the end of HFD feeding, with normalization to the body weight (kg0.75) (n = 8:8). (J) Schematic diagram of the construction of the homologous rs1421085_C knock-in (KIES) mouse model with homologous recombination of locus targeting in murine embryonic stem (ES) cells. (K to L) Body weight (K) and body composition (l) of KIES mice and WT littermates under HFD challenge initiating from 8-week-old to 23-week-old (n = 12:13). Data are mean ± s.e.m. of biologically independent samples; unpaired two-sided Student's t-test. * P < 0.05, ** P < 0.01. ns, not significant.

Figure 2

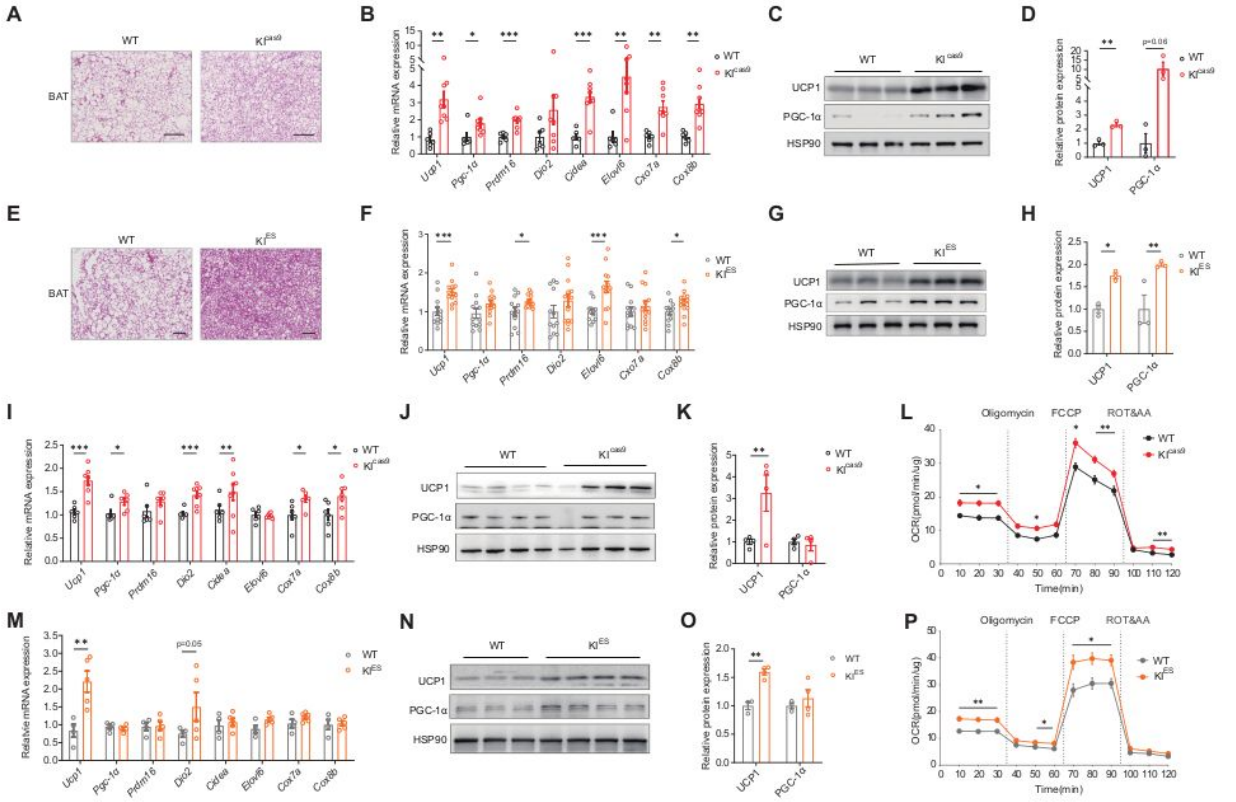

Figure 2

The homologous rs1421085 T>C variant augments thermogenic capacity of brown adipocytes. (A to D) The representative image of H&E staining (A), the mRNA expression of thermogenesis-related genes (B), the protein levels (C) and the qualification analysis (D) of UCP1 and PGC-1α in BAT of KIcas9 and WT mice under HFD (B, n = 11:16; C, D, n = 3:3). (E to H) The representative image of H&E staining (E), the mRNA expression of thermogenesis-related genes (F), the protein expression (G) and the qualification analysis (H) of UCP1 and PGC-1α in BAT of KIES and WT mice under HFD (F, n = 12:13; G H, n = 3:3). (I to L) The mRNA expression of thermogenesis-related genes (I), the protein expression (J) and qualification analysis (K) of UCP1 and PGC-1α, and oxygen consumption rate (OCR) (L) in the induced mature brown

adipocytes derived from BAT SVF of KIcas9 and WT mice (I, n = 4:6; J, K, n = 4:4; L, n = 4:5). (M to P) The mRNA expression of thermogenesis-related genes (M), the protein expression (N) and qualification analysis (O) of UCP1 and PGC-1α, and oxygen consumption rate (OCR) (P) in the induced mature brown adipocytes derived from BAT SVF of KIES and WT mice (M, n = 4:6; N, O, n = 3:4; P, n = 4:5). (A, E) Scale bar, 100 μm. Data are mean ± s.e.m. of biologically independent samples; unpaired two-sided Student's t-test. * P < 0.05, ** P < 0.01, *** P < 0.001.

Figure 3

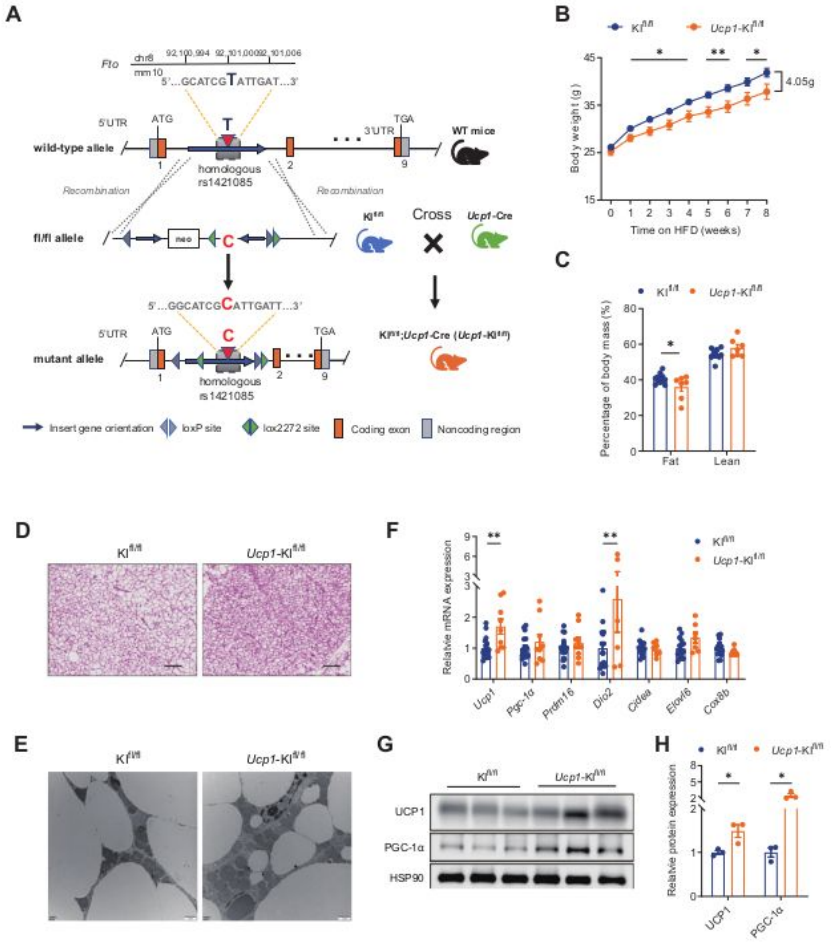

Figure 3

Brown adipocyte-specific knock-in of homologous rs1421085 T>C variant enhances thermogenesis and resists HFD-induced adiposity. (A) Schematic diagram of the genetic manipulation and construction of homologous rs1421085 variant knock-in mouse model (KIfl/fl; Ucp1-Cre, termed as Ucp1-KIfl/fl). (B to C) Body weight (B) and body composition (C) in Ucp1-KIfl/fl mice and KIfl/fl littermates under HFD challenge initiating from 9-week-old to 17-week-old (B, n = 12:7; C, n = 8:7). (D to H) Representative images of H&E staining (D) and TEM images (E), the mRNA expression of thermogenesis-related genes (F), the protein levels (G) and quantification analysis (H) of UCP1 and PGC-1α in BAT of Ucp1-KIfl/fl mice and KIfl/fl littermates under HFD. (D) Scale bar, 100 μm; (E) Scale bar, 1 μm. n = 3:3 in (D), (E), (G) and (H); n = 7:17 in (F). Data are mean ± s.e.m. of biologically independent samples; unpaired two-sided Student's t-test. * P < 0.05, ** P < 0.01.

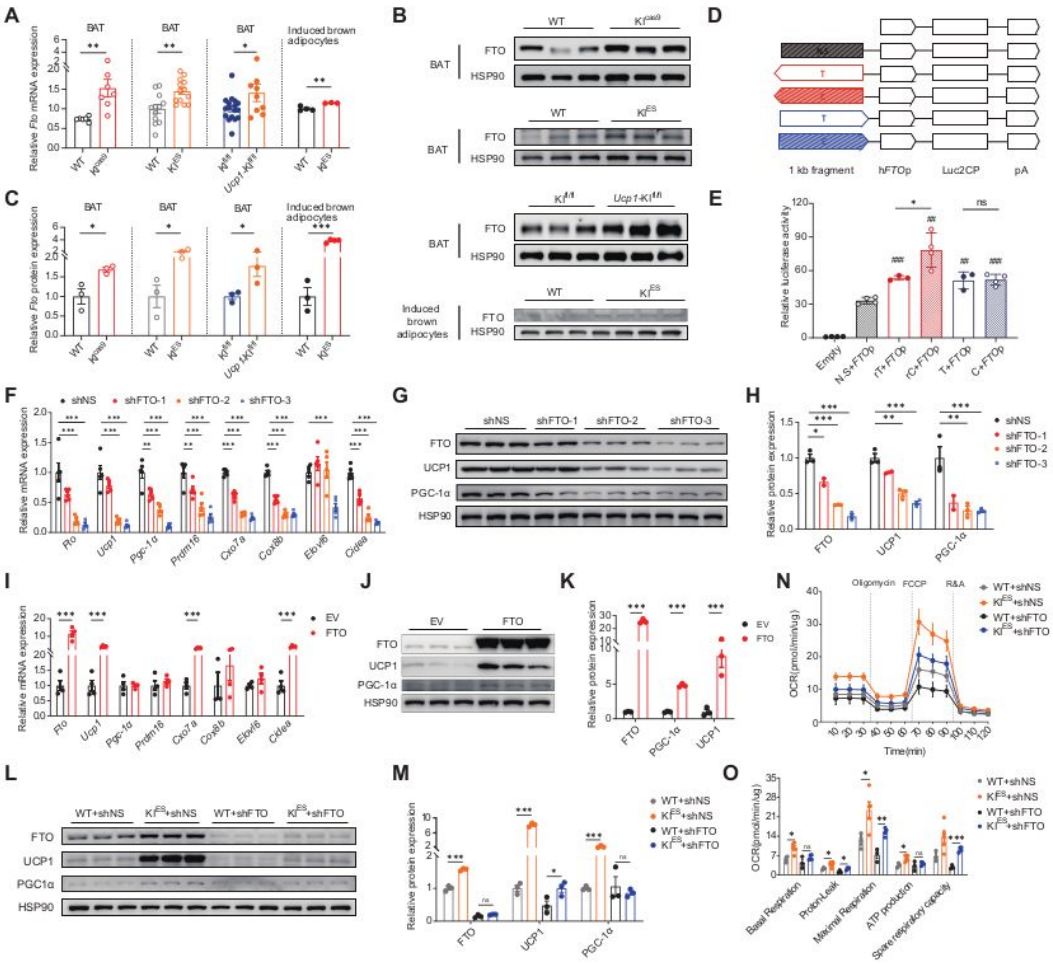

Figure 4

Figure 4

The homologous rs1421085 T>C variant increases thermogenesis via upregulating Fto expression. (A) The mRNA expression of Fto in BAT or mature brown adipocytes of indicated models (KIcas9, n = 6:7; KIES, n = 12:13; Ucp1-KIfl/fl, n = 17:9; induced brown adipocytes derived from KIES, n = 4:3). (B and C) The protein expression (B) and quantification analysis (C) of FTO in BAT or mature brown adipocytes of indicated models (n = 3:3 in BAT, n=3:4 in induced brown adipocytes). (D and E) The 1 kb region centered

on rs1421085 T>C variation was linked ahead of human FTO promoter (hFTOp) fragment and was subsequently fused to Luc2CP reporter gene (D). Luciferase activity was measured in HEK293T cells transfected with indicated plasmids, in which Renilla luciferase activity (E) was used for normalization (n = 3–4). pA, SV40 polyA; ns, not significant. ##, P< 0.01; ###, P < 0.001 compared with N.S.+ FTOp. (F to H) The mRNA expression of thermogenesis-related genes (F), the protein expression (G) and quantification analysis (H) of FTO, UCP1 and PGC-1α following Fto knockdown in induced mature brown adipocytes derived from BAT SVFs of C57BL/6J mice (MOI = 50; n = 2–4). (I to K), The mRNA expression of thermogenesis-related genes (I), the protein expression (J) and quantification analysis of FTO, UCP1 and PGC-1α (K) after overexpressing FTO in differentiated SVFs derived from BAT of C57BL/6J mice (MOI = 75; n = 2–4). (L to O) The protein expression (L) and quantification analysis (M) of FTO, UCP1 and PGC-1α, as well as OCR (N, O) after Fto knockdown in induced mature brown adipocytes derived from BAT SVFs of wild-type and KIES mice (MOI = 50; n = 3–4). Data are mean ± s.e.m. of biologically independent samples; unpaired two-sided Student’s t-test. * P < 0.05, ** P < 0.01, *** P < 0.001.

Figure 5

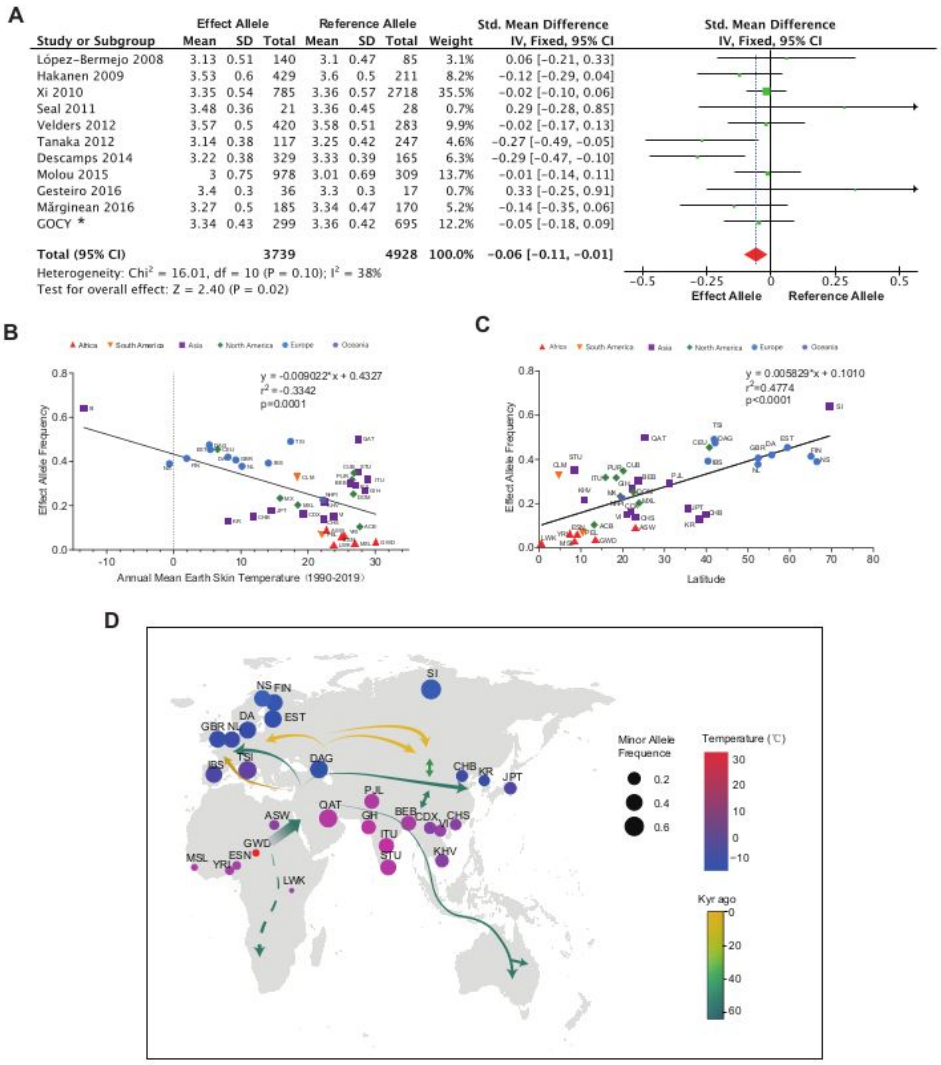

Figure 5

The rs1421085 T>C variant is associated with lower body weight of human infants and its allele frequency parallels with latitudes and ambient temperature of population distribution. (A) The Forest plot of the association between birth weight and human FTO rs1421085 polymorphism. Studies or subgroups included from previous studies and our in-home data were represented (see Methods). The size of the green box corresponding to each study was proportional to the sample size, while the horizontal line

showed the corresponding 95% confidential intervals (CI) of the standard deviation (std) mean difference. The overall std mean differences were based on a fixed-effects model shown by the red diamonds. The solid, vertical line represented the null result. *, data from the Genetics of Obesity in Chinese Youngs (GOCY) study. Effect allele, rs1421085_C; reference allele, rs1421085_T. SD, standard deviation, IV, inverse variance methods. (B and C) Correlation analysis of the effect allele frequency and absolute latitude (B) or annual mean earth skin temperature (C). Colors and symbols represented populations from different continents. (D) The relative proportion of the Africa-Eurasia populations carrying rs1421085_C allele. Each circle represented a distinct population: color means earth skin temperature, and size means rs1421085_C allele frequency. Arrows indicated the direction of population migration, and color represents the time of occurrence., Population details in (B) to (D) see table S5.

Supplementary Files

This is a list of supplementary files associated with this preprint. Click to download.

- SupplementaryMaterials.docx